The Effect of SVC-FACTS Controller on Power System Oscillation Damping Control

Ghazanfar Shahgholian[1], Seyed Mohsen Mirbagheri[1], Hosein Safaeipoor[1], Mehdi Mahdavian[2]
[1] Najafabad Branch, Islamic Azad University, Esfahan, Iran
[2] Naein Branch, Islamic Azad University, Esfahan, Iran
shahgholian@iaun.ac.ir

Abstract — Static var compensator (SVC) is used to improve the dynamic stability of the system using supplementary control. In this paper, dynamic behavior of the SMIB power system with SVC has been investigated. The gains of controller were selected based on a pole-placement technique. The IEEE type-ST1 is used for excitation system and the SVC is modeled by a controllable susceptance. Several simulations have been done to show the effect of the proposed approach to damping controller on power system oscillation stability.

I. INTRODUCTION

Power system damping controllers such as power system stabilizer (PSS) and FACTS based stabilizers may be used to damp dynamic oscillations and increase damping of the swing modes. PSS increases damping torque of a generator by affecting the generator excitation control, while FACTS devices improve damping by modulating the equivalent power-angle characteristic of the system [1].

Dynamic application of FACTS controllers includes dynamic stability, voltage stability enhancement and transient stability improvement. Among FACTS controllers, the shunt controllers have shown feasibility in term of cost effectiveness in a wide range of problem-solving from transmission to distribution levels. In principle, all shunt-type controllers inject additional current into the system at the point of common coupling.

The SVC is the most widely used FACTS device in power system regulation. It usually installs in power transmission systems and serves in various ways to improve the system performance. SVC is an effective and economical means of solving problems of transient stability, system reliability, static voltage stability, dynamic stability and steady state stability in long transmission lines [2, 3].

Many papers have been published in the field of damping control for power system oscillation by FACTS controller [4-7]. A systematic approach for designing of SVC based damping controllers for damping of low frequency oscillations in a SMIB power system is presented in [8]. In [9] discusses and compares different control techniques for damping undesirable inter area oscillation in power systems by means of power system stabilizers, SVC and STATCOM. The simultaneous coordinated tuning of the FACTS POD controller and the conventional PSS controllers in multi-machine power systems is presented in [10], which the linearized system model and the parameter-constrained nonlinear optimization algorithm is used. A hybrid genetic algorithm method to solve optimal power flow to select the best control parameters to minimize the total generation fuel cost and keep the power flows within the security limits in power systems incorporating FACTS is presented in [11].

FACTS controller helps to controlling both real and reactive power, which in addition to this control could provide an excellent tool for improving power system dynamics. This paper is proposed the dynamic simulation of the SMIB power system equipped with SVC based on mathematical modeling. A control strategy namely power oscillation damping (POD) of the SVC is also presented to improve damping of the low frequency oscillations. Eigenvalues and eigenvectors are used to examine the stability of the power system.

II. SYSTEM MATHEMATICAL MODEL

A. SVC Model

The main circuit of a SVC is shown in Fig. 1. It consists of four components: a fixed capacitor, bypass inductor, bidirectional thyristor valve and control system. The SVC can be operated in voltage regulation mode and in var control mode. It is capable of injecting controllable reactive power to bus where it is connected.

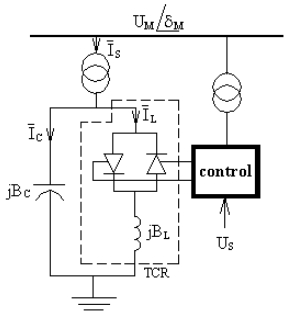

Fig. 1. The main circuit of SVC

TCR is a variable inductive reactor controlled by the firing angle α. The equivalent reactance of the TCR, $X_V(\alpha)$, at fundamental frequency is given by [12]:

$$X_V(\alpha) = \frac{\pi X_L}{2(\pi - \alpha) + \sin 2\alpha} \quad (1)$$

where X_L is the fundamental frequency reactance of the reactor without thyristor control. For the range of 90° to 180° of α,

$X_V(\alpha)$ start vary from actual reactance X_L to infinity. The conduction angle σ of the TCR depends on the α. The valves turn off automatically at the zero crossing of the ac current.

A SVC can be modeled by a variable shunt susceptance. It can be made to generate or absorb reactive power by means of thyristor controlled elements. The relationship between σ and stead state value of the susceptance of the SVC is given as follows:

$$B_E(\sigma) = \frac{1}{X_C} + \frac{\sin\sigma - \sigma}{\pi X_L} \tag{2}$$

where X_C is the reactance of the shunt capacitor and $\sigma=2(\pi-\alpha)$. The limits of the SVC are given by the firing angle limits, which are fixed by design.

The V-I characteristic is show in Fig. 2. It is specified by three operating regions: SVC is in regulation range, SVC is fully capacitive and SVC is fully inductive [13]. The reference voltage U_R is the voltage at the terminal of the SVC when it is neither absorbing nor generating any reactive power. The susceptance of the capacitor (slope of OA) is B_C and the susceptance of the reactor (slope of OBC) is B_L. The slope of the control characteristics is X_{SL}. A positive value of X_{SL} reduces the rating of a SVC.

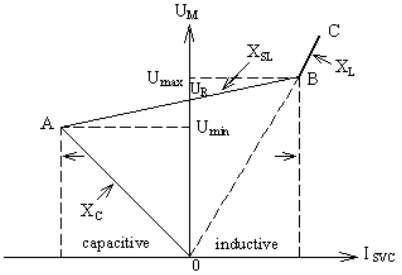

Fig. 2. Voltage–current characteristics of the SVC

The limits of the controller are given by the firing angle limits, which are fixed by design. Fig. 3 depicts the values of the susceptance of the SVC for different values of firing angle α, for compensation ratio λ=2, 3, 4. Notice that there is a value of angle critical (α_r) that causes steady-state resonance. For the SVC, resonance is not a problem, as it is shunt connected to the system and, hence, at the resonant point the controller is basically switched off the system without any notable effects.

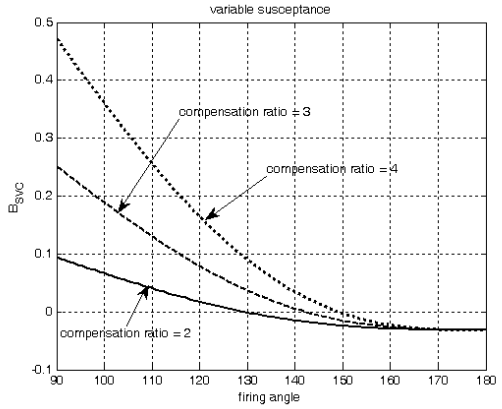

Fig. 3. Equivalent susceptance

Fig. 4 show the critical angle of SVC response for compensation ratio variations, from 2 to 4. We can see the α_r is between 129.3957° to 149.1471°.

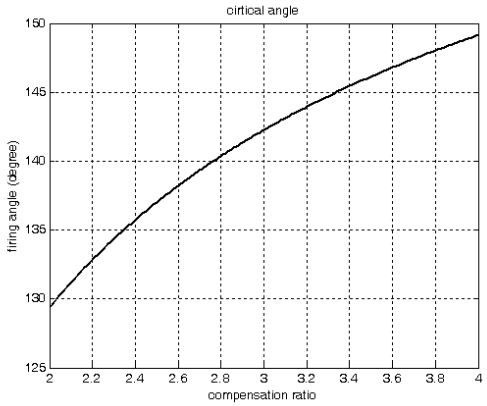

Fig. 4. Critical angle

B. System Equation

The system model for stability analysis is usually that of a SMIB power system. The configuration of the SMIB with SVC used in this study is shown in Fig. 5. The equivalent circuit is show in Fig. 6, where the transfer reactance between terminal machine and the infinite bus, X_T, is as follows:

$$X_T = X_S + X_R - B_E X_S X_R \tag{3}$$

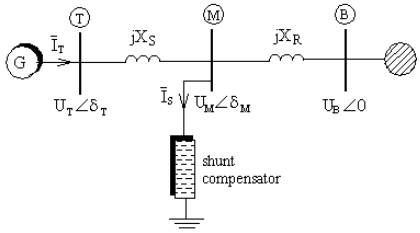

Fig. 5. SMIB power system with SVC

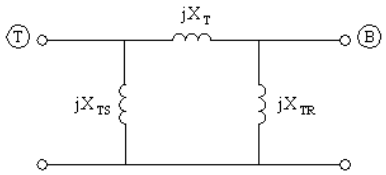

Fig. 6. The equivalent circuit

Using the variables defined in SMIB system the following equations can be written:

$$\bar{I}_T = \frac{(1 - X_2 B_E)\bar{U}_T - \bar{U}_B}{jX_T} \tag{4}$$

The power system dynamic model can be written as a set of differential equations and a set algebraic equation. The nonlinear dynamics of the SMIB system installed with SVC is given by following set of differential equations, where the dynamics of the generator is expressed in terms of the second order electromechanical swing equation and the internal voltage equation, the exciter by three first order differential equati-

ons and the SVC is modeled as controllable susceptance by a first order differential equation. Damping effects due to damper winding and rotor body eddy currents are neglected:

$$\begin{aligned}
&\frac{d}{dt}\delta = \omega_o \omega \\
&\frac{d}{dt}\omega = \frac{1}{2H}(P_M - P_E - K_D\,\omega) \\
&\frac{d}{dt}E'_q = \frac{1}{T'_{do}}[E_F - E'_q + (X'_d - X_d)\,i_d] \\
&\frac{d}{dt}E_F = -\frac{1}{T_A}E_F + \frac{K_A}{T_A}(U_T - U_R)
\end{aligned} \tag{5}$$

where δ is rotor angle, E'_q is the machine internal voltage, X'_d and X_q are the direct and quadrature reactance of the generator.

The active electrical power delivered by the generator is expressed as:

$$P_E = \frac{E'_q\,U_B}{X_D}\sin\delta - \frac{U_B^2\,(X_q - X'_d)}{2\,X_D X_Q}\sin 2\delta \tag{6}$$

where X_D and X_Q are given by:

$$\begin{cases} X_D = X_T + X'_d\,(1 - X_R B_E) \\ X_Q = X_T + X_q\,(1 - X_R B_E) \end{cases} \tag{7}$$

The stability can be improved by operating the SVC in inductive (B_E<0) or capacitive (B_E>0) mode. So the improve the dynamic performance of the system is achieved by the control of the susceptance of the compensator (B_E), which changes the electrical power output.

C. System Linear Model

The linearized model of the power system including SVC about an equilibrium operating point is used for small signal analysis and damping controller design. It can be obtained by linearizing equations for i_d and i_q around an operating point and then substituting in non-linear equation of the system. The d and q components of generator current of SMIB system installed with SVC can be expressed as:

$$\Delta i_q = \underbrace{\frac{U_B \cos\delta_o}{X_{QO}}}_{K_{qd}}\Delta\delta + \underbrace{\frac{I_{qo} X_2 X_q}{X_{QO}}}_{K_{qc}}\Delta B_E \tag{8}$$

$$\Delta i_d = \underbrace{-\frac{U_B \sin\delta_o}{X_{DO}}}_{K_{dd}}\Delta\delta + \underbrace{\frac{1 - X_2 B_{CO}}{X_{DO}}}_{K_{de}}\Delta E'_q$$

$$+ \underbrace{\frac{X_2\,(I_{do} X'_d - E'_{qo})}{X_{DO}}}_{K_{dc}}\Delta B_E \tag{9}$$

Figure 7 shows the block diagram representation of the small signal performance of the SMIB installed with a SVC. $G_V(s)$ is the exciter transfer function, $G_F(s)$ is the field circuit transfer function and $G_M(s)$ is the dynamic machine transfer function.

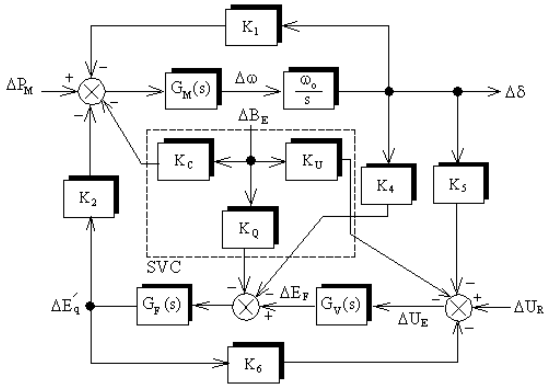

Fig. 7. Linearised dynamic model of the SMIB power system with SVC

D. Controller Design

The effectiveness of the SVC in enhancing small-signal stability depends on the location of the SVC, input control signals used, and controller design. The structure of the SVC controller with control loop is shown in Fig. 8.

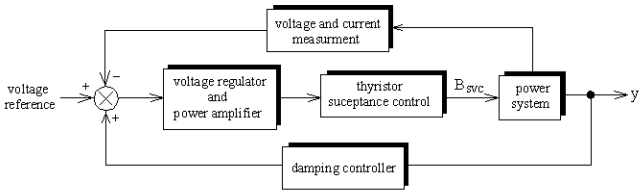

Fig. 8. Block diagram of the SVC controller

An SVC with firing control system can be represented by a first order model characterized by a gain K_R and time constant T_R as shown in Fig. 9. The input signal of the controller is the speed deviation and the output signal is the susceptance offered by the SVC. The control signal U_S is the added modulation signal of SVC for damping control and B_{CR} is a reference signal which is initial value of the SVC. The limits of the controller are given by the firing angle limits, which are fixed by design. Due to fast switching characteristics of thyristors, the time constants of an SVC device are very small. The susceptance of the SVC could be described by:

$$\frac{d}{dt}B_C = \frac{K_R}{T_R}(B_{CR} - U_S) - \frac{1}{T_R}B_C \tag{10}$$

The structure of POD controller has a similar structure to that of the power system stabilizer controller as shown in Fig. 10. The transfer function of the POD controller is given by:

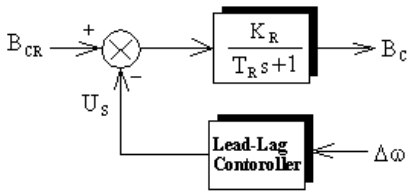

Fig. 9. Block diagram of the SVC control model

$$G_P(s) = K_P \frac{T_W s}{1+T_W s}\left(\frac{1+T_1 s}{1+T_2 s}\right)\left(\frac{1+T_3 s}{1+T_4 s}\right) \tag{11}$$

where K_P is positive constant gain and T_W is the washout time constant. T_1 and T_2 are the lead and lag time constant of leas-lag block, respectively.

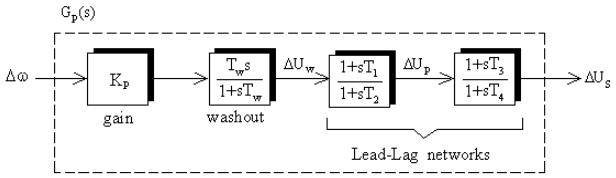

Fig. 10. POD controller

The POD controller is modeled by state-space analytical equations:

$$\frac{d}{dt}\Delta U_W = -\frac{K_P K_1}{J_M}\Delta\delta - \frac{K_P K_D}{J_M}\Delta\omega - \frac{K_P K_2}{J_M}\Delta E'_q - \frac{1}{T_W}\Delta U_W + \frac{K_P}{J_M}\Delta P_M \tag{12}$$

$$\frac{d}{dt}\Delta U_P = -\frac{K_P K_1 T_1}{J_M T_2}\Delta\delta - \frac{K_P K_D T_1}{J_M T_2}\Delta\omega - \frac{T_1 K_P K_2}{J_M T_2}\Delta E'_q + \left(\frac{1}{T_2} - \frac{T_1}{T_2 T_W}\right)\Delta U_W - \frac{1}{T_2}\Delta U_P + \frac{K_P T_1}{J_M T_2}\Delta P_M \tag{13}$$

$$\frac{d}{dt}\Delta U_S = -\frac{K_P K_1 T_1 T_3}{J_M T_2 T_4}\Delta\delta - \frac{K_P K_D T_1 T_3}{J_M T_2 T_4}\Delta\omega - \frac{T_1 T_3 K_P K_2}{J_M T_2 T_4}\Delta E'_q + \frac{T_3}{T_4}\left(\frac{1}{T_2} - \frac{T_1}{T_2 T_W}\right)\Delta U_W + \frac{1}{T_4}\left(1 - \frac{T_3}{T_2}\right)\Delta U_P - \frac{1}{T_4}\Delta U_S + \frac{K_P T_1 T_3}{J_M T_2 T_4}\Delta P_M \tag{14}$$

III. Simulation Results

The SMIB system is implemented for the simulation studies with and without the controller. Simulation results are presented for a SMIB power system using data in Table I.

Table II summarizes the value of the sensitivity constants with normal loading. In this case, the eiegnvalues of the system are: -0.0997, -2.0744, -5, -12.6740, -21.0923, -83.0952 and -1.5861±j4.2618.

Table III summarizes the value of the sensitivity constants with heavy loading. In this case, the eiegnvalues of the system are: -0.0999, -2.0355, -5, -18.9530, -22.4732, -77.3181 and -0.6640±j8.8558.

The system response for a step increase in mechanical power input with normal loading show in Figs. 11-14.

The system response for a step increase in mechanical power input with heavy loading show in Figs. 15-18.

TABLE I
Power System Parameter

Generator
J_M=10, X_q=1.7, X_d=1.8, X'_d=0.23, K_D=0, T'_{do}=8, f=60
Transmission line
X_S=0.5, X_R=0.5
Static var compensator
K_R=1, T_R=0.05
Normal loading
P_{Eo}=1, Q_{Eo}=0.015, U_{To}=1.05
Heavy loading
P_{Eo}=1.1, Q_{Eo}=0.4, U_{To}=1.05
Exciter
K_A=200, T_A=0.01

TABLE II
Sensitivity Constants of Model Power System with Normal Loading

Constant	Value	Constant	value
K_1	1.5998	K_{ic}	0.5851
K_2	0.4481	K_{id}	0.1621
K_3	1.1603	K_{ie}	-0.0740
K_4	-0.7035	K_{dc}	-0.1926
K_5	1.4704	K_{qd}	0.9978
K_6	0.5641	K_{dd}	-0.4481
K_{de}	-0.0880	K_{qc}	1.3828

TABLE III
Sensitivity Constants of Model Power System with Heavy Loading

Constant	Value	Constant	value
K_1	2.8683	K_{ic}	0.2718
K_2	0.3893	K_{id}	0.1521
K_3	1.1603	K_{ie}	-0.0806
K_4	-0.6111	K_{dc}	-0.2292
K_5	1.6243	K_{qd}	1.2698
K_6	0.7039	K_{dd}	-0.3893
K_{de}	-0.0880	K_{qc}	1.2012

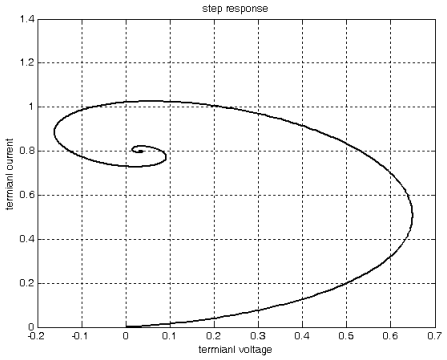

Fig. 11. Characteristic of voltage-current of the generator terminal with normal loading

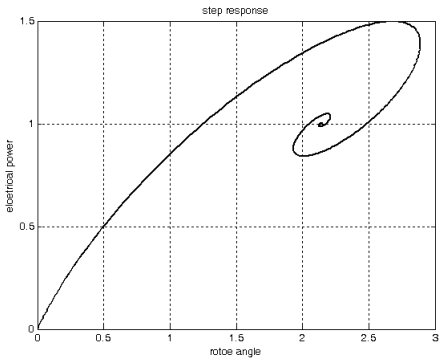

Fig. 12. Power-angle curve with normal loading

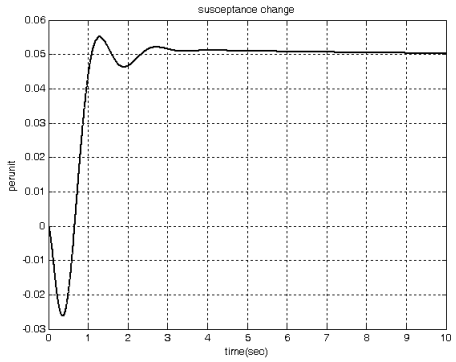

Fig. 13. Variation in susceptance of SVC with normal loading

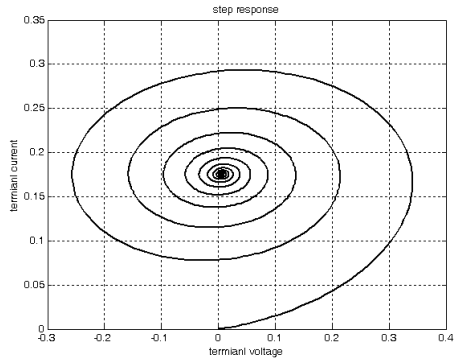

Fig. 14. Characteristic of voltage-current of the generator terminal with heavy loading

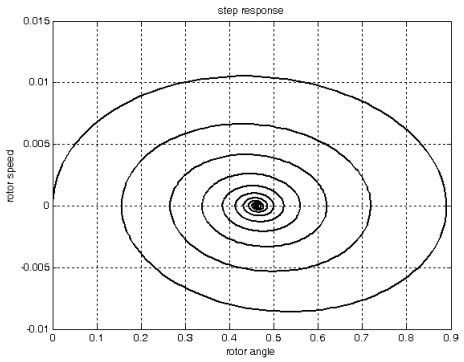

Fig. 15. Power-angle curve with heavy loading

Simulation results indicated that the SVC can significantly improve system damping. Based on the time domain results, it is obvious that at normal loading is a better option as it damp out oscillation faster than heavy loading.

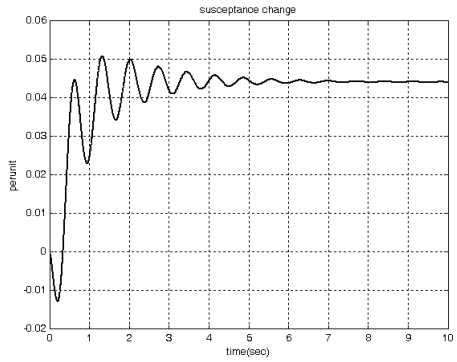

Fig. 16. Variation in susceptance of SVC with heavy loading

IV. CONCLUSION

SVC is used to damp out power system oscillations. The function of the SVC is either to inject reactive power to bus or to absorb reactive power from the bus where it is connected. The small signal stability can be improved by SVC.

Simulation results show that it can indeed improve the damping of the power systems. An eigenvalue-based objective function to increase the system damping ratio was developed.

REFERENCES

[1] G. Shahgholian, J. Faiz, "Static synchronous compensator for improving performance of power system: A review", *Int. Rev. of Elec. Eng.*, Vol.4, No.2, pp., Oct. 2010.

[2] A. Luo, Z. Shuai, W. Zhu, Z. J. Shen, "Combined system for harmonic suppression and reactive power compensation", *IEEE Tran. on Ind. Ele.*, Vol.56, No.2, pp.418-428, Feb. 2009.

[3] E. Zhijun, D.Z. Fang, K.W. Chan, S.Q. Yuan, "Hybrid simulation of power systems with SVC dynamic phasor model", *Elec. Pow. and Ene. Sys.*, No.31, pp.175–180, 2009.

[4] X. Lei, E.N. Lerch, D. Povh, "Optimization and coordination of damping controls for improving system dynamic performance", IEEE Trans. Pow. Sys., Vol.16, pp.473-480, Aug. 2001.

[5] R.H. Adware, P.P. Jagtap, J.B. Helonde, "Power system oscillations damping using UPFC damping controller", IEEE/ICETET, pp.340-344, Nov. 2010.

[6] H.Wang, "A unified model for the analysis of FACTS devices in damping power system oscillations – part III: unified power flow controller", IEEE Tran. On Pow. Del., Vol.15, No.3, pp.978-983, July 2000.

[7] P.K. Dash, S.Mishra, G.Panda, "Damping multimodal power system oscillation using a hybrid fuzzy controller for series connected facts devices", IEEE Tran. On Pow. Sys., Vol.15, pp.1360-1366, 2000.

[8] V.K. Chandrakar, S.N. Dhurvey, S.C. Suke, "Performance comparison of SVC with POD and PSS for damping of power system oscillations", *IEEE/ICETET*, pp.247-252, Nov. 2010.

[9] N. Mithulananthan, C.A. Canizares, J. Reeve, G.J. Rogers, "Comparison of PSS, SVC, and STATCOM controllers for damping power system oscillations", *IEEE Tran. On Pow. Sys.*, Vol.18, No.2, pp.786-792, May 2003.

[10] L.J. Cai, I. Erlich, "Simultaneous coordinated tuning of PSS and FACTS damping controllers in large power systems", *IEEE Tran. on Pow. Sys.*, Vol.20, No.1, pp.294-300, Feb.2005.

[11] T.S. Chung, Y.Z. Li, "A hybrid GA approach for OPF with consideration of FACTS devices", *IEEE Pow. Eng. Rev.*, pp.47-57, Feb. 2001.

[12] S. Biansoongnern, S. Chusanapiputt, S. Phoomvuthisarn, "Optimal SVC and TCSC placement for minimization of transmission losses", *IEEE/ICPST*, 2006.

[13] N. Sabai, H. Nandar Maung, T. Win, "Voltage control and dynamic performance of power transmission system using static var compensator", *Worl. Acad. of Sci., Eng. and Tec.*, pp.425-429, 2008.